INTERNATIONAL JOURNAL OF INTEGRATED ENGINEERING
ISSN: 2229-838X e-ISSN: 2600-7916

IJIE

Vol. 16 No. 7 (2024) 135-147
https://publisher.uthm.edu.my/ojs/index.php/ijie

The Effect of Different Diameter Rotor Bars Size on Performance of 0.5 Hp Induction Motor

Yanawati Yahya[1]*, Muhammad Khairul Hisyam Jarail[2], Dina Maizana[3], Ibrahim Alhamrouni[1], Mohd Badrulhisham Ismail[1]

[1] *Electrical Engineering Section, British Malaysian Institute, Universiti Kuala Lumpur, Gombak, 53100, MALAYSIA*
[2] *PETRONAS FLOATING LNG 1 (L) LTD., Block B, Level, Lot R-8 Riverson Suites, Kota Kinabalu, 88100, MALAYSIA*
[3] *Department Teknik Elektro, Universitas Medan Area, INDONESIA*

*Corresponding Author: yanawati@unikl.edu.my
DOI: https://doi.org/10.30880/ijie.2024.16.07.013

Article Info

Received: 25 June 2024
Accepted: 10 September 2024
Available online: 2 December 2024

Keywords

Induction motor, rotor bar diameter, rotor core, flux density, efficiency

Abstract

Induction motors are currently the most widely used industrial motors. In the field of industry, its self starting, tiny size, light weight, excellent effectiveness, minimal maintenance requirements, and simplicity to operate, less prone to accidents, and low cost per same power rating make it suitable for use. A fractional horsepower to thousands of horsepower is available. Induction motors can be found in centrifugal pumps, conveyors, compressor crushers, drilling machines, fans, blowers, escalators, refrigerators, and electric vehicles. In Malaysia, industrial motors consume 48% of total energy. In many industrialized countries, electric motors consume over 70% of the total energy. This study examines 4-pole, 0.5-hp, 50Hz, and 415V industry low-voltages 3-phase induction motors. Changing the diameter of the rotor bars is used to research how to increase the effectiveness of energy. The work proposed a new rotor design with modified bar sizes. This research was conducted utilizing two techniques: MATLAB programme simulation and theoretical calculation. Simulations show that the new design is significantly more energy efficient. The theoretical calculation was done using MATLAB. Through MATLAB programme, the effectiveness of the three rotor bar diameters and the suggested new model were compared. The finding indicated that the rotor bars with 0.648-inch diameters have a batter efficiency of 79.66% as compared to others with different diameters. Based on the simulation, the smaller the diameter of the rotor bar is more effective relative to the bigger rotor bar diameter based on a decent range of maximum rotor core flux density, which is less than 1T. The result is proven using MATLAB.

1. Introduction

The performance of the 0.5 Hp, 3 Phase Motor was adversely affected by the use of rotor bars with varying sizes, resulting in reduced energy efficiency. Differences in rotor bar size led to variations in current and power use, causing decrease power factor and efficiency. The research proposes a new rotor design with customized rotor bar diameter and an emphasis on optimizing flux distribution effects. The study discusses the potential benefits and challenges associated with implementing the new rotor bar size or diameter in industrial applications. This

suggests that improving energy efficiency through innovative rotor design can be beneficial but may come with certain challenges. The study demonstrates that a significant expanse of power can be spared by using high efficiency motors in industrialized applications. Specifically, changing rotor bars diameter resulted in a 4.5% higher efficiency compared to standard industry motors. This improvement helps reduce motor losses and, consequently, energy consumption. The rotor bar design with different diameters is stated to be applicable to motors of various horsepower ratings, indicating its versatility for a range of industrial machinery. The research also proposes a maintenance strategy for faulty motors, which is designed to minimize energy consumption, motor losses, and flux distribution issues. This strategy is suggested for implementation in various machinery.

Nikola Tesla created the induction motor around 1888. Induction motors in all engine applications are used effectively, except for the application that required extremely high torque or perfect variable speed control. Comprises induction motor, induction frequency converter, induction phase converters and electrical slip coupling is a revolving system of induction motor. This involves connection of electrical to the rotor, which is rotated by using a magnetic induction from or known as the stator [1].

A number of different variables such as output power, losses, efficiency, residual torque, current etc. necessity to be tackled. Due to its very easy to handle, powerful, reliable and cheap features is the reason why three-phase induction motor were used [2]. At approximately constant speed, the induction motor will operate from zero to full load. Electrical devices are so complicated that high precision and losses can almost hard to be expected [3]. The loss of rotor and stator copper, core metal, stray and load, and resistance and winding are five categories of induction motor failures or losses. The next losses known as stray losses, from a lack of precision between predicted and measured losses. The key element in the device were losses of the rotor and stator [3].

An electric motor is a system used to convert electrical energy to mechanical energy. Motors can run at multiple voltages either in one or in three phase, of DC or AC supply. Three phase alternating current function shows that it is a combination of 3 single phase with different starting angle as shown in Fig. 1. Hence, as seen in Fig. 2, the peak voltages are similarly separated apart the induction motor's 3-phases is easy to maintain, simple, inexpensive [4].

The function of the 3-phase induction motor is following Lorentz Force and the Faraday's law that applied to the winding. As other motors, an induction motor has a fixed outside section which is known as stator, and rotor rotates carefully inside the motor and has air gap between both rotor and stator. The stator part generated by rotating magnetic field, caused by the rotor part's alternate emf and current [4].

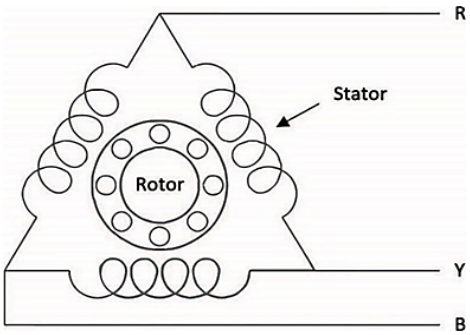

Fig. 1 *Fundamental of 3-phase induction motor*

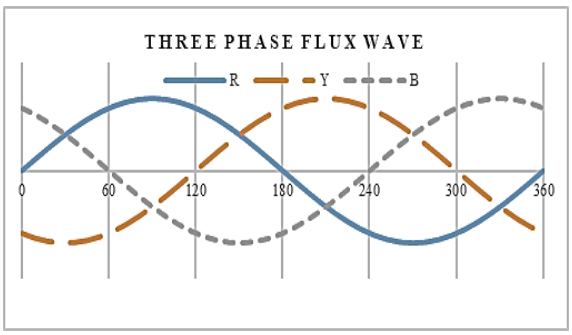

Fig. 2 *Fluxes of three phase waveform*

The shapes are similar to the squirrel cage and because of that, this type of induction motor namely squirrel cage. Both shows the instantaneous path of the stator flux as it travels through between the rotor at separate periods. The arrows at the centre of rotor in Fig. 3 represent the instantaneous direction of the resulting flux. Fig. below show the concepts of squirrel cage induction motor's rotor part [5].

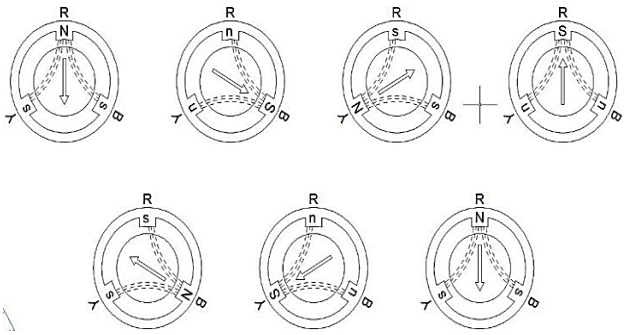

Fig. 3 *Regulation of resulting stator flux*

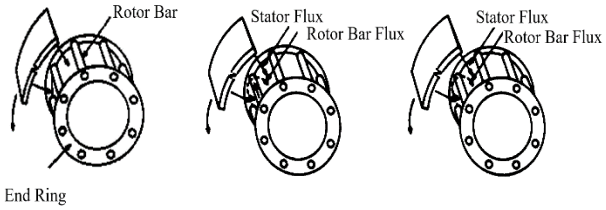

Fig. 4 *Rotor flux and rotation*

Int. Journal of Integrated Engineering Vol. 16 No. 7 (2024) p. 135-147

Fig. 4 shows the rotor field slipping in the counterclockwise direction of the rotor bar. Under Lenz's law, the relative movement between the rotor bar material and the magnetic field, which is directed at opposing the relative movement creating voltage, current and flux. This is due to the flux produced by the rotor bar always in clockwise direction [6].

To interpret the construction of the 3ϕ Induction Motor, two key sections in the induction motor must be understood as a fundamental aspect. A 3ϕ Induction Motor involves of two elements which is stator and rotor [7]. The rotor segment is mounted inside the stator component with a slight air gap between 0.4 mm and 4 mm depending on the strength of the induction motor as shown in Fig. 5. Although, as an outcome of the residual surface barrier to the domain wall, the comparison of hysteresis losses for 0.50 mm and 0.35 mm sheets is still high loss of hysteresis with low sheet thickness barrier to the domain wall flow as seen in Fig. 6. Fig. 6 shows the field lines of Phase Transformer (Left) and Motor (Right) [8].

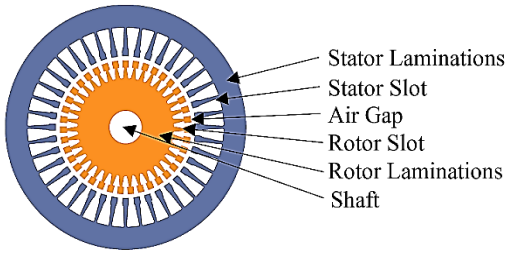

Fig. 5 *The view of stator laminations, stator slot, air gap, rotor slot, rotor lamination, and shaft*

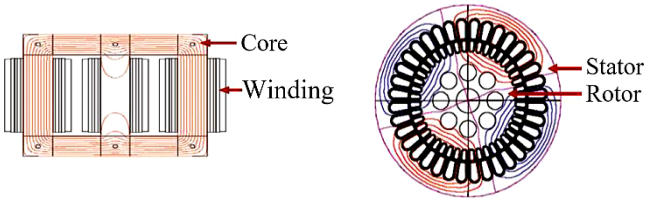

Fig. 6 *Field lines of phase transformer (left) and motor (right)*

The inner coupling of the three-phase induction motor with the symbols L1, L2 and L3, represent the network phases, was carried out and correspondingly connected to terminals U1, V1 and W1. The construction of lamination of rotor and stator for the rotor bars and stator teeth slot [8].

The length, shape, cross sectional area and bar of the rotor surface define the characteristics of the rotor. Due to its excellent conductivity and low cost, aluminium was selected as the typical rotor bar alloy in induction machines to satisfy ecological, metallurgical, and mechanical requirements, as well as its good molecular structure. Since copper has more than 60% lower conductivity than aluminium, a costlier copper content is a recommendation for rotor bars. over the past two decades in order to pursue better effectiveness [9].

Code letter was given on the nameplate of the motor to indicates type of bars used to build a rotor. It can be divided into four rotor form classes as seen in Table 1 [10].

Table 1 *Rotor bars slot type [10]*

Design of Rotor Bars Slot	Descriptions / Characteristics
A	The design has a larger rotor bars, so a high starting current with a moderate starting torque is expected.
B	The design was a standard design for industrial motor. This design has average starting torque and moderate starting current.
C	▪ The design consists two shapes (for two different sizes and type of rotor bars) that are linked together. ▪ The small part of the bar will give the high starting torque while the deeper section will reduce the slip. ▪ The design has moderate starting current.
D	The design was presently barely for loads that require a high initial torque, but low torque near rated speed.

In addition, some of the induction engines have a good start-up, and operating characteristics have been complete based on the form of the rotor bars. This rotor bar form can be split up into three classes, which are a double cage, a deep slot and a standard cast aluminium rotor slot. A deep-bar rotor required less starting current, high starting torque and even running resistance, proves that it can rally the necessary starting and running performance. In addition, rotor structure is made of 2 elements, which is of bars and the end-ring that connected in short circuit [10].

Flux density focuses on a rotor bar's flux density distribution finite-element frame. The dynamic and stationary study of the system is done for squirrel cage rotor bar. Results demonstrate that variations in the flux

density of the rotor bar have a direct affect on the machine's overall efficiency. In consequence, any distortion of the flux density arises from the poor design of rotor bars [11].

In order to design the efficient motor starter and meet the requirement of customer, the manufacturer have to be equipped with a specific load requirement. Simulations of these motors using MATLAB tools were subsequently carried out to develop an induction motor and a permanent magnet cylindrical brushless AC motor. For normal working conditions, the reason of this simulation is to analyse effect of various diameter with the distribution of the flux distribution of motor. Improving the power factor as well as the efficiency of induction machines is one of the key element to save energy, even a minor enhancement in performance will save significant energy. Table 2 indicates the performance when the motor system is divided to various types of rotor bars in stable and adjacent rotor bars. Because rotor bars are divided into 2, the efficiency tends to increase for most rotor bar classes, but when divided into 3 bars, there is a small decline in efficiency. As shown in Fig. 7, the rotor bars shape has been designed based on Table 2 [12]. The induction motor configuration specification for each of two types of rotor bars of the same thickness as shown in Fig. 8. Moreover, the rotor bar is fitted with such a higher in locked rotor torque and slip [13].

Table 2 *Rotor bar for type 1, 2, 3, 4 and 5 [12]*

Rotor Bar Type	Healthy	1 Broken Bar	2 Broken Bar	3 Broken Bar
	η (%)	η (%)	η (%)	η (%)
Type 1	76.189	72.511	74.914	74.732
Type 2	75.054	75.484	75.752	75.664
Type 3	76.923	77.331	77.534	77.424
Type 4	78.129	78.441	78.668	78.609
Type 5	77.003	79.668	79.752	77.556

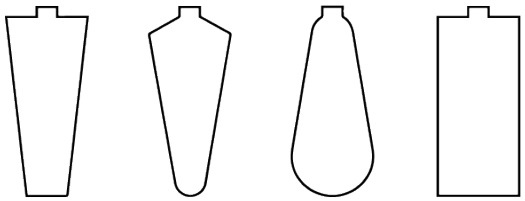

Fig. 7 *Rotor bar shapes design (a) Type 2; (b) Type 3; (c) Type 4; and (d) Type 5*

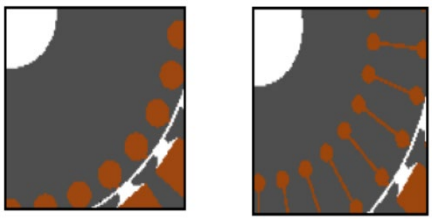

Fig. 8 *Design of round bars (left) and round outer and inner bars (right) of rotor bar [13*]

The induction motor works at synchronous speed during mechanical loading. In addition, graphs of slip, rpm, power factor, input power, strength, stator current, and output power presents the induction motor equivalent circuit performance. Likewise, the effectiveness of the performance variables of the induction motor with regard to the identical circuit parameters at three separate output powers [14].

And the analysis shows the impact of each circuit parameter on input power, power factor, maximum torque, speed, output power, stator current efficiency, and starting current respectively. Induction motor performance including loss mechanism is characterized as the supply of three-phase electrical voltages and currents to an induction motor, the induction motor test phenomenon and the loss of eddy current and hysteresis [15].

Since there is no supply linked with the rotor of an induction motor, the only power supply for the rotor would be the electricity that passes through the air gap in form of magnetic before it is converted into electrical form. The average power that passes through the air gap should be equal to the amount of losses of dissipated ohmic rotor coil as heat energy and the power will be converted into mechanical energy [16].

The losses of induction motor are normally split into, rotor loss, stator loss, core loss, and rotational loss. All the losses mentioned are called traditional losses. The other losses that are not mentioned are depending on the connection of the motor, which is harmonic loss [17]. Performance parameters of the motor, such as air gap length, influence magnetic current, power factor, performance of overload, noise and temperature [18]. Usually, the output torque and rotational speed of an induction motor are closely linked to air gap. In the configuration and optimization of the induction motor, the flux density must be considered [19]. Based on characteristics of flux density as shown in Fig. 9 below, when a flux density is increase more than 1 T, the efficiency will decrease due to high loss and unsmooth flux density [20].

Int. Journal of Integrated Engineering Vol. 16 No. 7 (2024) p. 135-147

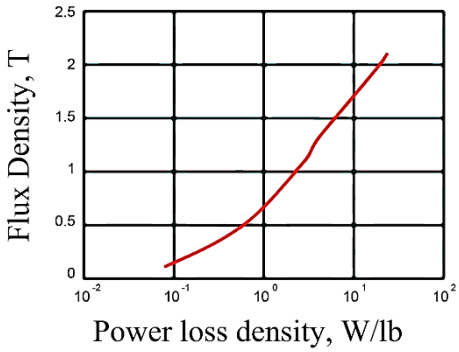

Fig. 9 *Characteristics of flux density against power loss density*

A relationship between losses, flux density of rotor cores, and efficiency has been found. By substituting the equation, the result will be as follows:

$$Efficiency, \eta = \frac{P_{OUT}}{P_{IN}} \times 100\% = \frac{P_{IN} + P_{CORE\ LOSS}}{Hp\ \times 746} \times 100\% \quad (1)$$

Where η is the efficiency, P_{OUT} and P_{IN} is power out ant power in, $P_{CORE\ LOSS}$ is power losses and Hp is Horsepower (For this research, 0.5 Hp are applied).

$$B_{rcm} = \frac{\emptyset_m}{(D_r - D_{sh}2d_{r1})l_a SF} \quad (2)$$

Where B_{rcm} is maximum rotor tooth flux density, D_{sh} is shaft diameter, l_a is stator lamination stack length, D_r is rotor diameter, d_{r1} is rotor slot depth, and SF is stacking factor. To get a better flux result, a B_{rcm} value should be in good range (less than1T). If the maximum flux distribution rate of rotor core is more than 1T then based on Fig. 9, we need to reduce the rotor slot depth's value [20].

To evaluate the impact of different air gaps (0.3 mm, 0.5 mm, and 1.0 mm), three induction motor (IM) models with equivalent electrical properties were investigated in this work. Two unique motors with different diameters were included in the variants, together with a standard 1.5 kW wye-connected motor operating on three phases. Using Finite Element Analysis, the torque, efficiency, and ripple parameters were calculated. Comparing the other types' relative efficiency (94% and 92%), the kind with a 1.0 mm air gap performed worse (88.4%) [21].

At 1360 rpm, the largest power factor of 0.97 was recorded at 0.3 mm, while lower power factor values of 0.92 and 0.95 were noted at 0.7 mm and 1.0 mm gaps, respectively. The magnetising current increased from 3 to 4.36 A, losses from 73.7 to 91.4 W, and torque ripples from 4.15% to 4.74% when the air gap was increased. For optimal dependability and effectiveness, the air-gap thickness should be between 0.3 and 0.5 mm. Air gaps should be minimised by induction motor designers in order to improve power factor and lower no-load losses [22].

The performance of induction motors has been studied in several recent research. A modified winding function method was used in [23] to analyse the performance of a three-phase induction machine with an axial non-uniform air-gap, or static eccentricity. In a similar vein, [24] examined eccentricity in three-phase induction motors using geometries to evaluate electromagnetic torque and inductances in order to improve performance. Based on core magnetic properties, the operational performance of a 1.5 kW induction motor was assessed in [25] using a 2D electromagnetic model. Additionally, [26] used the torque and stator current temporal harmonics as well as the variation of the magnetic field in the middle circle of the air-gap to assess the performance of 3-phase, 5-phase, 7-phase, and 9-phase squirrel cage induction motors.

In summary, this work highlights the importance of optimizing rotor bar size in induction motors to enhance energy efficiency, reduce losses, and improve overall motor performance. The findings indicate that such improvements can have a positive impact on energy conservation and industrial operations. Additionally, the applicability of the proposed rotor bar design and maintenance strategy to various motor sizes and machinery makes it a valuable contribution to industrial energy efficiency practices.

To have the capability of being able to increase the induction motor's efficiency, research and analysis were done on squirrel-cage induction motors by changing the diameter or size of the rotor bars. The techniques applied involve theoretical calculations that are resolved by MATLAB simulation. The simulation will be used for the investigation and evaluation of induction motors. MATLAB software has been used in this study as a simulation programme. The aim of design simulations and mathematical calculations is to give the results of a comparison between three rotor bar diameters in terms of induction motor effectiveness improvement.

2. Methodology

The works and techniques used in the work are explained in this subtopic. For this investigation, the several methods are used to do the performance analysis on the 0.5Hp Induction Motor for different rotor bars diameter which are MATLAB software simulation and theoretical calculation. Fig. 10 shows the flowchart of a research project in designing the rotor bars part with various diameter. Based on the flow chart, firstly the 0.5-Hp 3-phase motor design will be reviewed by reading the journal, books, online article and other related articles. The aim of this project is to make a Induction Motor rotor with excellent performance and high effectiveness.

Secondly, the simulation and comparison are started using MATLAB software. The setup for the coil winding, stator, and overall features are fixed variables. The rotor configuration is the variable being changed, and the induction motor's output is the variable being adjusted to. In the rotor setting, variables such as bar diameter are altered. The modelling process is carried out until the induction motor exhibits good efficiency, flux distribution, and loss performance.

Besides that, a calculation for the efficiency and flux transfer by changing rotor bars diameter in this research project will be calculated and compared. The idea of this calculation is to show the simulation result. It can conclude that the research work of the performance of motor rotor part is designed with better efficiency and flux distribution in range value. To start this research, a proper stage needs to be taken so that this study can be conducted accordingly. All these stages are stated in the research framework as shown in Fig. 10.

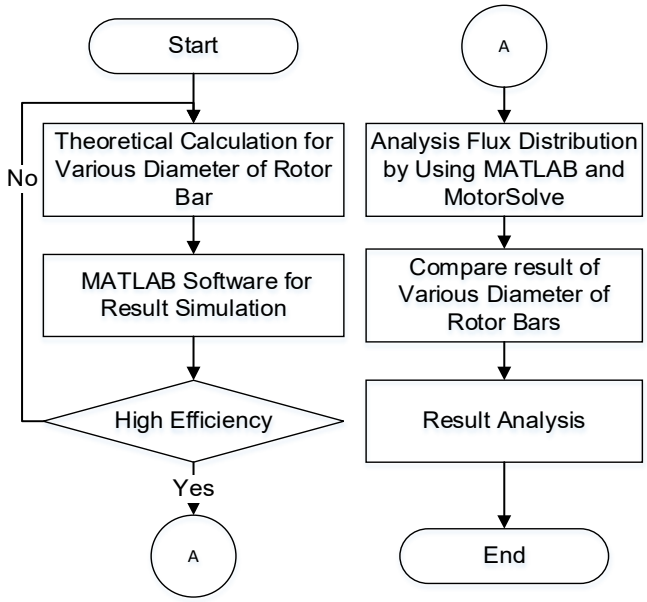

Fig. 10 *Flowchart of research framework*

Fig. 11 shows parameter d_{r1} represented rotor bar diameter in the calculation, where it will affect the maximum flux density of rotor core B_{rcm}. In this theoretical calculation, parameters based on the real value of induction motors were used, such as: V_L = 420 V, P_S = 0.5 Hp, Speed = 1400 rpm, f_{req} = 50 Hz, a = 1, Thickness of Frame (t_f) = 0.35 mm, P = D_f = 4.3125 inch. As shown in Fig. 12, the NEMA Basic Dimension parameters has been designed based on Table 3.

Table 3 *NEMA quick guide table for stator and rotor of induction motor designs*

NEMA FRAME		D	E	2F	P	U	V	AB
Inch	48	3	1.875	1.25	4.3125	0.5	0.5	3.625
mm		76.2	47.625	31.75	109.5375	12.7	12.7	92.075

Int. Journal of Integrated Engineering Vol. 16 No. 7 (2024) p. 135-147

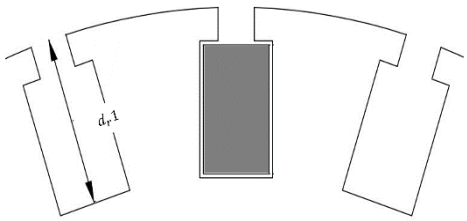

Fig. 11 *Rotor slot section view*

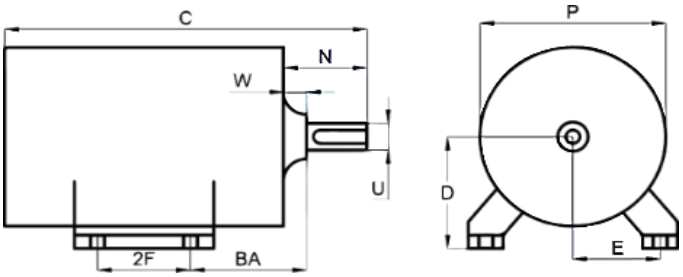

Fig. 12 *NEMA basic dimension*

First process will be design the different rotor bars diameter then simulate by using MATLAB software. The efficiency result of different diameter of rotor bars will be collected by calculation and simulation. This part is to identify the efficiency and flux distribution when using a different rotor bars diameter in 0.5 Hp induction motor.

This MATLAB software simulation reads the data file system known as Pc.m, imeval.m and imdesign.m, which contains general descriptive motor dimension data and insert all the calculated data to the data file. For mesh as shown in Fig. 13 and contour as shown in Fig. 14, first to do is design a Z-axis matrix for both mesh and contour plotting for all diameter of rotor bars according to the value of flux density. Below is example for ¼ pole of 0.348 inch rotor bars diameter.

0.00	0.00	0.02	0.02	0.02	0.02	0.02	0.02	0.02	0.02	0.02	0.02	0.02	0.00	0.00
0.00	0.02	0.06	0.06	0.06	0.06	0.06	0.06	0.06	0.06	0.06	0.06	0.06	0.02	0.00
0.02	0.06	0.10	0.10	0.10	0.10	0.10	0.10	0.10	0.10	0.10	0.10	0.10	0.06	0.02
0.02	0.06	0.10	0.14	0.14	0.14	0.14	0.14	0.14	0.14	0.14	0.14	0.10	0.06	0.02
0.02	0.06	0.10	0.14	0.18	0.18	0.18	0.18	0.18	0.18	0.18	0.14	0.10	0.06	0.02
0.02	0.06	0.10	0.14	0.18	0.25	0.45	0.45	0.45	0.25	0.18	0.14	0.10	0.06	0.02
0.00	0.02	0.06	0.10	0.14	0.18	0.25	0.25	0.25	0.18	0.14	0.10	0.06	0.02	0.00
0.00	0.00	0.02	0.06	0.10	0.14	0.18	0.18	0.18	0.14	0.10	0.06	0.02	0.00	0.00
0.00	0.00	0.00	0.02	0.06	0.10	0.14	0.14	0.14	0.10	0.06	0.02	0.00	0.00	0.00
0.00	0.00	0.00	0.00	0.02	0.06	0.10	0.10	0.10	0.06	0.02	0.00	0.00	0.00	0.00
0.00	0.00	0.00	0.00	0.00	0.02	0.06	0.06	0.06	0.02	0.00	0.00	0.00	0.00	0.00
0.00	0.00	0.00	0.00	0.00	0.00	0.02	0.02	0.02	0.00	0.00	0.00	0.00	0.00	0.00

Fig. 13 *Z-axis matrix for contour plotting of 10.16mm diameter of rotor bars*

0.00	0.00	0.00	0.00	0.00	0.45	0.45	0.45	0.45
0.00	0.00	0.00	0.00	0.45	0.25	0.18	0.18	0.18
0.00	0.00	0.00	0.45	0.18	0.14	0.14	0.14	0.14
0.00	0.00	0.45	0.25	0.18	0.10	0.10	0.10	0.10
0.00	0.00	0.45	0.18	0.14	0.10	0.06	0.06	0.06
0.00	0.45	0.25	0.18	0.14	0.10	0.06	0.02	0.02
0.00	0.45	0.18	0.14	0.10	0.10	0.02	0.02	0.02
0.00	0.45	0.18	0.14	0.10	0.06	0.02	0.00	0.00
0.45	0.25	0.18	0.14	0.10	0.06	0.02	0.00	0.00

Fig. 14 *Z-axis matrix for mesh plotting of 10.16mm diameter of rotor bars*

Using the Z matrix value, the coding is added to the coding for graph plotting as explained in Fig. 15 and Fig. 16.

```
x=0:2:57;
y=0:2:57;
z= [0.00 0.00  0.00  0.00  0.00  0.00
        0.00  0.00  0.00  0.00  0.00
        0.00  0.00  0.00  0.00  0.00
        0.00  0.00  0.00  0.00  0.00
        0.00  0.00  0.00  0.00  0.00
        0.00  0.00  0.00
0.00    0.00  0.00  0.00  0.00  0.00
        0.00  0.00  0.00  0.17  0.17
        0.17  0.17  0.17  0.17  0.17
        0.17  0.17.....
```

Coding	Description
mesh(x,y,z);	Plot value x, y and z in mesh

xi=linspace(12,44,50); yi=linspace(12,44,50);
[xxi,yyi]=meshgrid(xi,yi);
zzi=interp2(x,y,z,xxi,yyi,'cubic');
	Set the figure to start from 12 to 40 to get only rotor flux and 0 to 53 to get the whole motor flux

pcolor(xxi,yyi,zzi), shading interp;
title ('Contour');
xlabel('X-AXIS [cm]');
ylabel('Y-AXIS [cm]');
	Create line axis, title and label to the figure

colorbar;	Insert colour bar for reference
hold on contour3 (xxi,yyi,zzi,12,'k'); hold off	Show result as contour with 12 numbers of flux lines

Fig. 15 *Coding for contour flux distribution*

```
x=0:2:37;
y=0:2:37;
z= [0.000.00  0.00  0.00  0.00  0.00
        0.00  0.00  0.00  0.00  0.00
        0.00  0.00  0.00  0.00  0.00
        0.00  0.00  0.00
    0.00      0.00  0.00  0.00  0.00
        0.00  0.92  0.92  0.92  0.92
        0.92  0.92  0.92  0.00  0.00
        0.00  0.00 ..........
```

Coding	Description
meshz(x,y,z);	Plot value x, y and z in mesh
xi=linspace(0,37,30); yi=linspace(0,37,30);	Set the figure to start from 0 to 37

[xxi,yyi]=meshgrid(xi,yi);
zzi=interp2(x,y,z,xxi,yyi,'cubic');
surf(xxi,yyi,zzi);
	Plot the mesh as surface to get a solid mesh surface instead of only mesh line

zlim([0.02 1.5])	Set the Z axis to start from 0.02 to 2
colorbar;	Insert colour bar for reference

title ('Mesh');
xlabel('X-AXIS [cm]');
ylabel('Y-AXIS [cm]');
zlabel('Flux Density [T]');
	Create line axis, title and label to the figure

Fig. 16 *Coding for mesh flux distribution*

3. Results and Discussion

In order to accomplish the objectives of this study, this topic highlights all the findings collected from data analysis. This work was built on the basis of research objectives for a regular 0.5 Hp induction motor using MATLAB software to ensure that the required output can be obtained for the efficiency of the diameter of rotor bars. In order to determine the behaviour and efficiency of the various rotor bar types, the effects of the different rotor bar data examined using the calculation and simulation process are also discussed. This section also points out the results and discussion on the production of various rotor bar diameters in terms of efficiency output enhancement and flux distribution. A 0.5 Hp squirrel cage induction motor performance evaluation with different

Int. Journal of Integrated Engineering Vol. 16 No. 7 (2024) p. 135-147

rotor bars diameter is presented. Simulation and theoretical calculation have been done with MATLAB Software for the Induction Motor's performance. In each design, the size of the rotor bars was changed.

Based on this study, able to apply different type of rotor bars used can be observed to see the effect on losses and distribution of flux is expected. When flux density is regulated smoothly (not more than 1T) (Jimmie & Stephan, 2001), efficiency can be improved and increased, and the desired result is reached as in Fig. 17. Upon simulation of MATLAB, the calculation and performance efficiency can be proven. When flux density is regulated smoothly and within the good range, efficiency can be improved and increased, and the desired result is reached. Upon simulation of MATLAB, the calculation and performance efficiency can be proven as shown in Fig. 17.

```
| Different Diameter Rotor Bars Size Effect |
|  on Performance of 0.5 Hp Induction Motor |

=========================================
  Maximum Value of Rotor Core Flux Density
=========================================
        Brcm (dr1 = 0.680) = 91.77
        Brcm (dr1 = 0.550) = 65.5759
        Brcm (dr1 = 0.348) = 45.4279

=========================================
         Efficiency in Percentage
=========================================
     Efficiency(dr1=0.680)(%) = 75.2662
     Efficiency(dr1=0.550)(%) = 78.6318
     Efficiency(dr1=0.348)(%) = 79.6635
```

Fig. 17 *MATLAB simulation result for rotor flux value*

Table 4 *The comparison of theoretical calculation and MATLAB simulation software in flux density*

Rotor Bar Diameter (inch)	Maximum value of rotor core flux density, (B_{rcm})	
	Theoretical Calculation	Simulation MATLAB
	Tesla (T)	
0.680	0.917490	0.917700
0.550	0.655607	0.655759
0.348	0.454170	0.454279

From the result in Table 4, the value of flux density then plotted into MATLAB simulation to see the flux density distribution along the rotor in contour and mesh view as shown in Fig. 18, Fig. 19 and Fig. 20 with different diameter of rotor bars. By referring to the colour bar, flux distribution with red colour is already exceed the maximum limit of flux density, which is exceed 100 kilolines/in^2 or 1T.

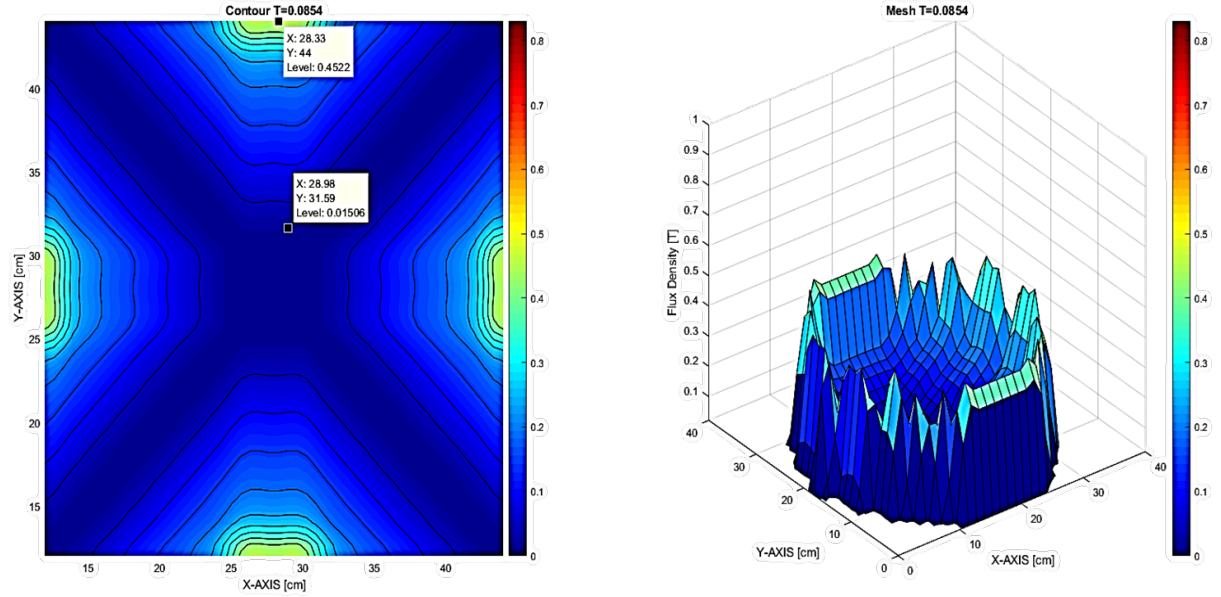

Fig. 18 *Contour and mesh graph of the flux distribution for 0.348 inch of rotor bars diameter*

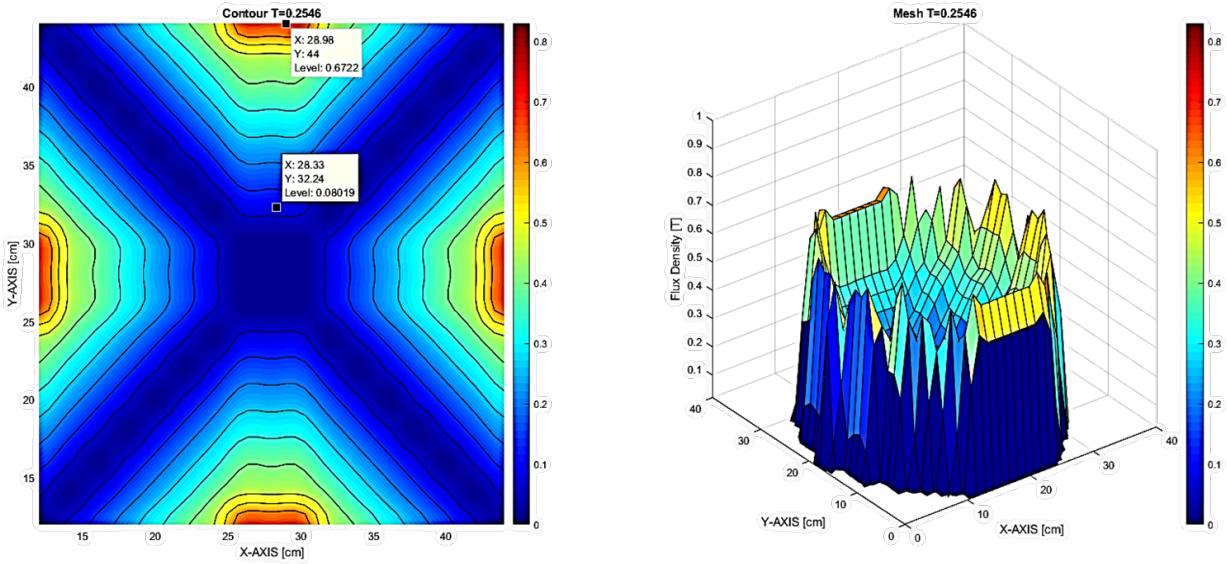

Fig. 19 *Contour and mesh graph of the flux distribution for 0.550 inch of rotor bars diameter*

Int. Journal of Integrated Engineering Vol. 16 No. 7 (2024) p. 135-147

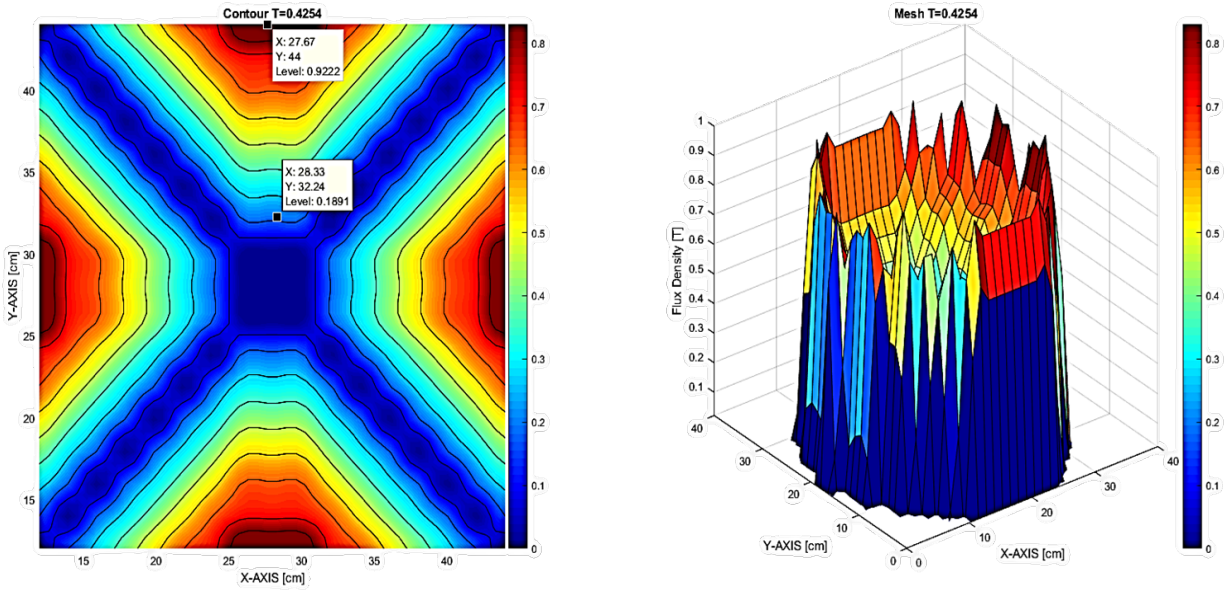

Fig. 20 *Contour and mesh graph of the flux distribution for 0.680 inch of rotor bars diameter*

Based on MATLAB simulation result in Fig. 17, it shows that 0.648 inch of rotor bars' diameter has the highest efficiency with 79.66 %, and as the result in Table 4 shows that none of the flux of the rotor is exceeding the maximum limit since the maximum flux is 0.45 T, which means not exceed the good range. Besides that, according to the Table 4 above, for 0.550 inch rotor bars diameter, it shows that the flux is higher than 0.648 inch's with the value of flux is 0.66T. Furthermore, for 0.680 inch of rotor bars diameter shows the lowest efficiency with 79.27% as refer to Fig. 17. When it plotted in mesh and contour in MATLAB Simulation, it shows some of the flux are close the maximum value.

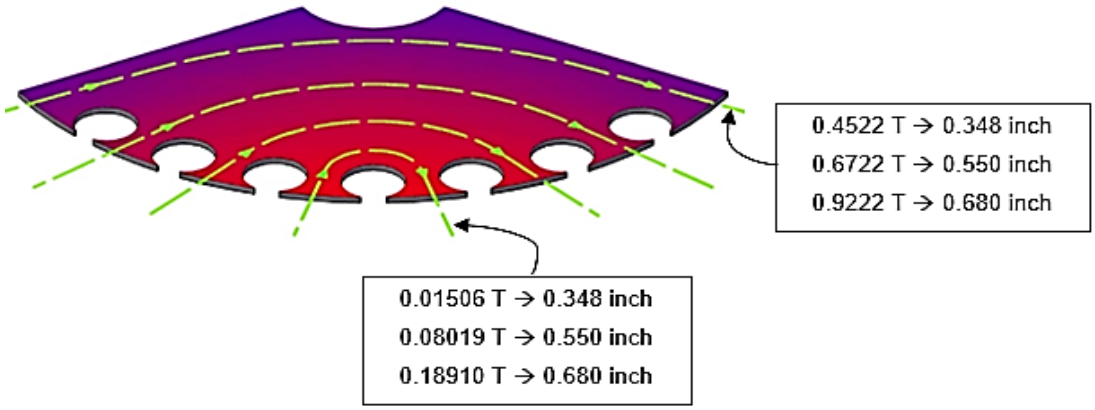

Fig. 21 *Flux distribution for all diameters of rotor bar*

Based on Fig. 21, the flux density value close to the shaft zone or known as inner diameter of rotor frame is smaller than the flux density distributed at rotor bar area or known as outer diameter of rotor frame. This is because the higher the reluctance and length, the weaker the flux density. The reluctance of magnetic circuit or section of a magnetic was released according to its length, correctional area (A) and permeability of material (μ). From this observation, it shows that the data from experimental is related and prove by a theoretically.

4. Conclusion

The goal of this experiment was to demonstrate how much energy could be saved by adopting high-efficiency motors. The estimate uses the suggested modification as a case study. In this study, analysis on the effect of the effect of different rotors bars diameter on flux distribution in 0.5 HP induction motor has been carried out by using three different sizes of rotor bars diameter which are 0.348-inch, 0.550 inch and 0.680 inch. Additionally, the difficulty and possible rewards of adapting the new layout for usage in factories were explored.

The investigation has shown that using highly efficient motors for motors in factories might result in significant energy savings. This study's new, different-diameter-designed rotor bar has proven to be 3.8% more

efficient than the previous diameters, which will lower the rate of motors failures. MATLAB was used to validate a number of computational findings for the suggested revised layout. Since the error amount is less than 6%, it can be shown that the mathematical MATLAB calculating demonstrates that the simulation's outcome from computation was adjusted. Analysis using simulation and statistical method with a mathematical calculation formula for diameter of the rotor bar has been done on the flux density checks. Based on the calculation, the rotor bars width has been tested to give the accuracy and precision of predicted data. Different value for the diameter, Dr1 shows that different diameter of rotor bars has a different value of flux density of induction motor. Furthermore, the design of this motor is applicable for any scale of motor horsepower. The suggested technique for fixing malfunctioning motors can be used on any type of machinery and will minimize energy use, motor losses, and carbon dioxide (CO2) released to the environment. Real-time estimation of its actual running loss is necessary for future study to accurately predict the trend in motor efficiency decline under various failure scenario.

Based on the study, the following recommendations can be implemented and taken out for development purposes: safety, which is it will produce the tripping alarm sensor to detect the leakage of broken rotor bar and warn by using IOT. To ensure that rotors with high performance can be made, the design and number of teeth must be enhanced. The material utilised will improve induction motor performance by increasing the material of the rotor bars to reduce losses and increase efficiency.

Acknowledgement

The authors would like to express their appreciation to the director and members of the Centre for Research and Innovation (CoRI), Universiti Kuala Lumpur (UniKL), for technical and financial assistance, as well as other members from PETRONAS and Universitas Medan Area, Indonesia, for technical and idea assistance.

Conflict of Interest

Authors declare that there is no conflict of interests regarding the publication of the paper.

Author Contribution

The authors confirm contribution to the paper as follows: ***study conception and design:*** *Yanawati Yahya, Muhammad Khairul Hisyam Jarail;* ***data collection:*** *Muhammad Khairul Hisyam Jarail;* ***analysis and interpretation of results:*** *Yanawati Yahya, Dina Maizana, Ibrahim Alhamrouni;* ***draft manuscript preparation:*** *Yanawati Yahya, Mohd Badrulhisham Ismail. All authors reviewed the results and approved the final version of the manuscript.*

References

[1] Y. Yanawati, N. H. Halim, I. Daut, S. Nor Shafiqin, I. Pungut, M. N. Syatirah and M. Abdullah, "Efficiency increment of 0.5hp induction motor by using different thickness of rotor lamination steel sheet via FEM," 5th International Power Engineering and Optimization Conference, PEOCO 2011, p. 188–192, 2011. DOI: 10.1109/PEOCO.2011.5970407.

[2] W. Theodore, "Electrical machines, drive and power systems (6th ed)," New Jercy: Pearson Prentice Hall, 2006.

[3] I. Daut, N. Gomesh, Y. Yanawati, M. Irwanto, S. Nor Shafiqin and Y. M. Irwan, "Modeling and Simulation of 0.5 HP rotating machine for the investigation of losses by using copper as rotor bar material," Australian Journal of Basic and Applied Sciences, pp. 5(12), 179–188, 2011. ISSN 1991-8178

[4] Y. Jianfeng, T. Zhang and Q. Jianming, "Electrical Motor Products," Woodhead Publishing Limited, 978-0-85709-077-5 (print) ISBN: 978-0-85709-381-3 (online), 2011. eBook - ePub

[5] I. H. Charles, "Principles of Three Phase Induction Machines. In Stephen (Second)," Electric Machines: Theory, Operation, Applications, Adjustment and Control, p. 133 – 136, 2002e.

[6] Y. Yanawati, "Design of 0.5 HP Induction Motor Rotor Bars with 0.35 mm and 0.50 mm Thickness of Steel Sheets for Rotor Fabrication," Thesis for the degree of Doctor of Philosophy UniMAP, pp. 9 -12, 16-43, 2016.

[7] D. S. Al-Oraini and I. B, "Book, Chapter Four Three Phase Induction Machine," 2010.

[8] TEC Electric Motors, "Motor Catalogue 2013," 2013, p. (1). www.tecmotors.co.uk. chrome-extension://efaidnbmnnnibpcajpcglclefindmkaj/https://www.electric-motors.online/_webedit/uploaded-files/All%20Files/TEC/TEC%20Motors%20-%20Motor%20Catalogue%202013%20-%20Issue%201.pdf

[9] H. J. Lee, S. H. Im, D. Y. Um and G. S. Park, "A Design of Rotor Bar for Improving Starting Torque by Analyzing Rotor Resistance and Reactance in Squirrel Cage Induction Motor," IEEE Transactions on Magnetics, pp. 54(3), 1–4, 2018. DOI:10.1109/TMAG.2017.2764525

[10] L. Herman Stephen, "Three Phase Motors. In Electrical Transformers & Rotating," ISBN:9780766805798, 0766805794. Delmar Publishers. Published: 1999, Digitized: August 25, 2009.

[11] D. P. Kothari and I. J. Nagrath, "Engineering Textbooks, Electric Machines (Fourth) McGraw Hill," 2010.

[12] E. Maloma, M. Muteba and D. V. Nicolae, "Effect of rotor bar shape on the performance of three phase induction motors with broken rotor bars," Proceedings - 2017 International Conference on Optimization of Electrical and Electronic Equipment, OPTIM 2017 and 2017 Intl Aegean Conference on Electrical Machines and Power Electronics, ACEMP 2017, p. 364–369, 2017. DOI: 10.1109/OPTIM.2017.7974997
[13] D. Maizana, Y. Yanawati and A. Nazifah, "Effect of different type of rotor bars on performance using FEM," pplied Mechanics and Materials, 679 (October 2018), p. 247 – 253, 2014. DOI:10.4028/www.scientific.net/AMM.679.247
[14] S. Indulkar and K. Ramalingam, "Sensitivity Analysis of Induction Motor," 2007. [Online]. Available: https://www.researchgate.net/ publication/ 242751687_ Sensitivity_Analysis_of_Induction_Motor_Performance.
[15] G. N. Shashidharan, "Design and Measurement of Losses in AC Induction Motor," Master Thesis Universiti Malaysia Perlis, 2009.
[16] H. Syahrain and Y. Yanawati, "The effect of different rotor bars type on flux and losses distribution in 0.5Hp induction motor," Thesis for the Bachelor of Engineering Technology (Hons.) in Electrical in UNIKL, pp. 14-17, 2020.
[17] Y. Xie and W. Cao, "Influence of broken bar fault on the performance of squirrel-cage induction motor at standstill.," 2011 International Conference on Electrical Machines and Systems, ICEMS 2011, 1–5., p. https://doi.org/10.1109/ICEMS.2011.6073626, 2011.
[18] Y. Yanawati, R. Khairil and H. Kadhim, "Improvement of Performance, Economy and Environment: Effects of Magnetic Flux Density on Rotor Bar Shape," International Journal of Renewable Energy and Engineering Research, 2020. https:// DOI: 10.13140/RG.2.2.11683.07208
[19] Y. Shuaichen and Y. Xiaoxian, "Fast analytical calculation of the air-gap flux density in an outer-rotor permanent-magnet brushless motor," MATEC Web of Conferences 189, 06008 MEAMT 2018, 2018. https://doi.org/10.1051/matecconf/201818906008
[20] J. C. Jimmie and W. Stephan, "Electrical Machines," Analysis and Design Applying MATLAB, pp. 375-404, 2001. ISBN 07-118970-X, McGraw Hill Series in Electrical and Computer Engineering.
[21] Onwuka, Ifeanyichukwu Obi, Patrick Oputa, Osita Ezeonye, Chinonso (2023a), “Performance Analysis of Induction Motor with Variable Air-Gaps using Finite Element Method”, NIPES Journal of Science and Technology Research, 5, pp 112-124, 2023. DOI: 10.5281/zenodo.7729203.
[22] Onwuka, Ifeanyichukwu Obi, Patrick Oputa, Osita Ezeonye, Chinonso (2023b), “Performance Analysis of Induction Motor with Variable Air-Gaps using Finite Element Method”, NIPES Journal of Science and Technology Research, 5, pp 112-124, 2023. DOI: 10.5281/zenodo.7729203.
[23] X. Li, Q. Wu and S. Nandi (2021). Performance Analysis of a Three-Phase Induction Machine with Inclined Static Eccentricity. IEEE Transactions on Industry Applications, Vol. 43(2), pp. 531-541.
[24] O. S. Olaleye, C. O. Ahiakwo, D. C. Idoniboyeobu and S. Orike (2022). Modeling of Eccentricity and Performance of Three-Phase Induction Motors. Journal of New views in Engineering and Technology (JNET),Vol. 2(1), pp. 97-108
[25] C. Ai, X. Cao and H. Wang (2021). Analysis of a 1.5kW Induction Motor Through Electromagnetic and Thermal Simulations. 3rd Asia Energy and Electrical Engineering Symposium, Chengdu, China, 26-29 March,2021, pp. 249-254.
[26] V. Fireteanu, A. Constantin and C. Dumitru (2021). Finite Element Analysis of the Performance of the 3-Phase, 5-Phase, 7-Phase and 9-Phase Squirrel-Cage Induction Motors. The 12th International Symposium on Advanced Topics in Electrical Engineering, Bucharest, Romania, 25-27 March, 2021, pp. 1-6.